Ecloud Build-Up Simulations for the FNAL MI for a Mixed Fill Pattern: Dependence on Peak SEY and Pulse Intensity During the Ramp*

M. A. Furman,† Center for Beam Physics, LBNL, Berkeley, CA 94720,
and CLASSE, Cornell University, Ithaca, NY 14853

Abstract

We present simulation results of the build-up of the electron-cloud density n_e in three regions of the FNAL Main Injector (MI) for a beam fill pattern made up of 5 double booster batches followed by a 6th single batch. We vary the pulse intensity in the range $N_t = (2-5)\times 10^{13}$, and the beam kinetic energy in the range $E_k = 8 - 120$ GeV. We assume a secondary electron emission model qualitatively corresponding to TiN, except that we let the peak value of the secondary electron yield (SEY) $\delta_{\max}$ vary as a free parameter in a fairly broad range.

Our main conclusions are: (1) At fixed N_t there is a clear threshold behavior of n_e as a function of $\delta_{\max}$ in the range $\sim 1.1-1.3$. (2) At fixed $\delta_{\max}$, there is a threshold behavior of n_e as a function of N_t provided $\delta_{\max}$ is sufficiently high; the threshold value of N_t is a function of the characteristics of the region being simulated. (3) The dependence on E_k is weak except possibly at transition energy.

Most of these results were informally presented to the relevant MI personnel in April 2010.

INTRODUCTION

The desire to assess the impact of the electron-cloud effect on the MI upgrade [1] has motivated the measurement of the incident electron flux J_e on the walls of the MI vacuum chamber by means of a RFA electron detector installed in a field-free region [2] for various high-intensity beam fill patterns [3], and of the measurement of the semi-local average of the volumetric electron-cloud density n_e by means of the microwave dispersion technique [4, 5].

In this note we present simulation results for n_e in three different regions of the chamber, which we label "edet," "bend," and "FFellip." The first one, "edet," represents a round-pipe field-free region where the RFA is installed. The other two represent regions where the microwave transmission measurements have been performed: "bend" represents a dipole bending magnet, and "FFellip" a field-free region, both having elliptical chamber cross section. Table 1 provides the assumed values for the relevant parameters.

In the exercises considered here vary E_k, bunch intensity N_b and $\delta_{\max}$ in the range specified in Table 2, but not in all possible combinations (here N_b is the bunch intensity in any of the first 5 batches; the bunch intensity in the 6th batch is always 50% of that in the first five). Detailed parameter values for each case are explained below. Preliminary results were presented at the PAC09 [6].

The results were obtained with the 2D program POSINST, which simulates the electron-cloud build-up and decay in a specific region of the chamber under the action of a prescribed beam fill pattern [7–10]. All results here are based on the simulation for only one full machine revolution; this is sufficiently long for the electron cloud to reach steady state, which typically occurs within the first ~ 2 μs following beam injection into an empty chamber.

ASSUMPTIONS

We assume a beam fill pattern similar to what has been used in the corresponding measurements, consisting of 6 batches in which the first 5 are obtained by slip-stacking booster batches; the 6th batch bunch intensity is 50% of that in any of the first five. Owing to an initial misunderstanding, we used two slightly different patterns for different sets of simulation runs (see Fig. 2). The difference in the results for these two is expected to be negligible; for the sake of the record, however, we specify in the results below which pattern was used in which case.

Although the beta functions and the transverse RMS beam sizes are different in the three sections, we set them equal for the purpose of the exercises carried out in this note. The bunch sizes quoted in Table 1 for $E_k = 8$ GeV correspond to a normalized 95% emittance $\epsilon_{95,n} = 15\times 10^{-6}$ π m-rad. For higher E_k we simply scale these σ's in proportion to $\gamma^{-1/2}$, where γ is the usual relativistic factor for the beam.

In actuality, the longitudinal bunch shape, at least in the first 5 batches, is fairly flat as a result of the stacking process; however, to simplify things, we have assumed that the shape is gaussian with an RMS bunch length (in time) $\sigma_t = \tau_{95}/4$, where τ_{95} is the 95% bunch duration plotted in Fig. 1. Simulations comparing gaussian vs. flat longitudinal bunch profiles for the LHC [11], as well as for the MI (unpublished), showed very small differences in similar parameter regimes. Finally, we have assumed that the three RMS bunch sizes are the same for all bunches in the ring.

The electron-cloud build-up is seeded by ionization of residual gas. The ionization electron creation rate (electrons generated per proton per unit length of beam traversal) quoted in Tab. 2 is computed from the formula

$$n'\ [\mathrm{m}^{-1}] = 3.284\,\sigma_i\ [\mathrm{Mbarn}] \times P\ [\mathrm{Torr}] \times \frac{294}{T\ [\mathrm{K}]} \quad (1)$$

* Work supported by the FNAL MI upgrade R&D effort and by the US DOE under contract DE-AC02-05CH11231.

† mafurman@lbl.gov

However, in essentially all cases, it is the secondary electron emission that dominates the intensity of the process. The model used here for the secondary electron emission spectrum corresponds, approximately, to that of TiN. However, we take $\delta_{\max}$ as a free parameter that we exercise in a fairly broad range. Ideally, by fitting the results obtained here to measurements, one might determine $\delta_{\max}$. The validity of this fit assumes, of course, that all other relevant parameters are frozen at some realistic value. While previous work indicates that the values of these other parameters are reasonably realistic, we have not checked the above assumption.

Essentially all the present results were informally presented to the relevant MI personnel in April 2010. This work amounts to a logical continuation of the studies initiated in early 2006 [12]. A complete publication list can be found in Ref. 13.

RESULTS

Build-up at fixed E_k

There is evidence that the electron cloud signal in the RFA has a significant dependence on E_k, peaking at $E_k \simeq 60$ GeV. On the other hand, it appears that the microwave dispersion measurements show a signal that is fairly independent of E_k except near transition at $E_k \simeq 20$ GeV [14]. Furthermore, the dispersion measurements have been studied in a bit more detail at 120 GeV, hence our choices $E_k = 60$ GeV for "edet,", and $E_k = 120$ GeV for "bend" and "FFellip."

Results for n_e as a function of time during one revolution period are shown in Figs. 4,5,6 for the 3 regions considered. Each of the 4 plots in each case corresponds to 4 different values of N_t, as indicated. The simulations for all three regions show a clear threshold of n_e as a function

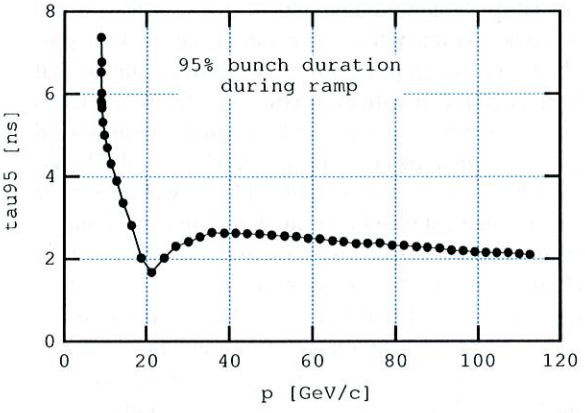

Figure 1: Measured 95% bunch duration during the ramp as a function of the beam momentum.

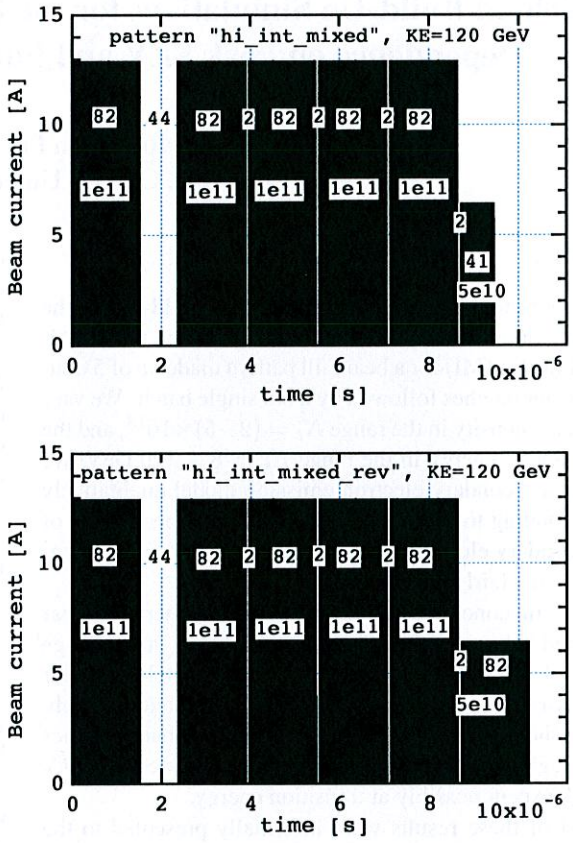

Figure 2: Fill patterns used in the simulations for one machine revolution, for the case $N_b = 1 \times 10^{11}$. The bottom numbers (1e11,...) represent the bunch population. The top numbers (82,44,...) represent the number of filled or empty buckets. Pattern "hi_int_mixed" has 451 bunches, "hi_int_mixed_rev" 492.

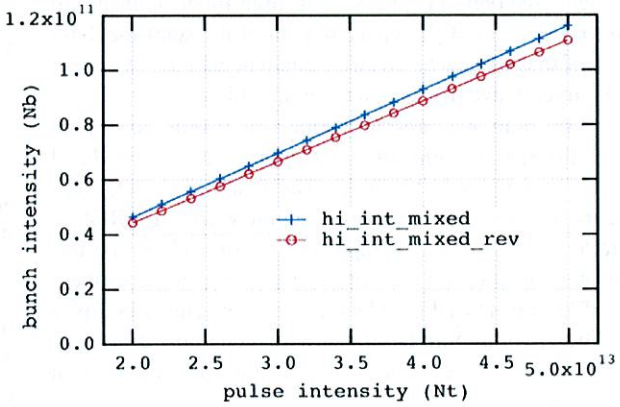

Figure 3: Bunch intensity in any of the first 5 trains as a function of total beam intensity for the two fill pattterns considered, shown in Fig. 2. The bunch intensity in the 6th train is always 50% of the value in any of the first 5 trains.

Table 1: Assumed local parameters in the three simulated regions.

quantity	symbol [unit]	"edet"	"bend"	"FFellip"
Beta functions	(β_x, β_y) [m]	(20, 30)	(20, 30)	(20, 30)
RMS transv. beam sizes at $E_k = 8$ GeV	(σ_x, σ_y) [mm]	(2.291, 2.806)	(2.291, 2.806)	(2.291, 2.806)
Pipe cross section	$\cdots$ [$\cdots$]	round	elliptical	elliptical
Pipe semiaxes	(a, b) [cm]	(7.3, 7.3)	(6.15, 2.45)	(6.15, 2.45)
Dipole field at $E_k = 8$ GeV	B [T]	0	0.1022	0

Table 2: Assumed global parameters.

Ring and beam	
Ring circumference	$C = 3319.419$ m
Revolution period at 120 GeV	$T_0 = 11.07\ \mu$s
RF frequency at 120 GeV	$f_{\rm RF} = 53.10$ MHz
Harmonic number	$h = 588$
Beam kinetic energy	$E_k = 8 - 120$ GeV
Bunch profile	3D gaussian
95% bunch duration	see Fig. 1
Pulse intensity	$N_t = (2 - 5) \times 10^{13}$
Bunch intensity	$N_b \simeq (0.4 - 1.1) \times 10^{11}$
Fill pattern	see Figs. 2 & 3
Primary e$^-$ sources	
Residual gas pressure	$P = 20$ nTorr
Temperature	$T = 305$ K
Ionization cross-section	$\sigma_i = 2$ Mbarns
Ionization e$^-$ creation rate	1.266×10^{-7} (e/p)/m
Secondary e$^-$ parameters	
Range of peak SEY	$\delta_{\rm max} = 0 - 1.7$
Energy at $\delta_{\rm max}$	$E_{\rm max} = 292.6$ eV
SEY at 0 energy	$\delta(0) = 0.2374 \times \delta_{\rm max}$
Simulation parameters	
Primary macroelectrons/bunch	1000
Max. no. of macroelectrons	20000
Full bunch length	$L_b = 5\sigma_z$
Integration time step	(1 or 2.5) $\times 10^{-11}$ s
Space-charge grid	64×64

of $\delta_{\rm max}$, and also that this threshold value depends clearly on N_t. This threshold dependence had already been noted earlier [15]. For $N_t > 4 \times 10^{13}$, the threshold in $\delta_{\rm max}$ is in the range 1.1–1.3. The region "edet" shows a weaker dependence on $\delta_{\rm max}$ than the other two, probably because its larger radius leads to lower electron-wall impact energies, hence to a lower effective SEY. However, when both $\delta_{\rm max}$ and N_t are above threshold, the steady-state value of $n_e \lesssim 1 \times 10^{12}$ m^{-3} is similar in all cases, corresponding to $\lesssim$100% beam neutralization. In these simulations we chose an integration time step $\Delta t = 1 \times 10^{-11}$ s which, based on prior experience, is sufficiently short to yield numerically stable results. The one-turn averaged n_e corresponding to the above build-up simulations are shown in Fig. 7 for the 3 regions considered, showing more clearly the threshold behavtior as a function of N_t for each value of $\delta_{\rm max}$.

The "bend" exhibits a non-monotonic behavior of $n_e(N_t)$ for $\delta_{\rm max} = 1.3$. This behavior has also been noticed in simulations for the proposed PS2 and for the SPS [16–18], although not yet experimentally verified. The non-monotonicity can likely be explained by the fact that, as N_t grows, the average electron-wall impact energy crosses $E_{\rm max} \simeq 293$ eV (where the SEY is maximum) when $N_t \simeq 3 \times 10^{13}$. This explanation makes sense only when the effective SEY is $< 1 (> 1)$ for $N_t < 3 \times 10^{13} (> 3 \times 10^{13})$, which is valid only for the trace corresponding to $\delta_{\rm max} = 1.3$ in Fig. 7. A full explanation remains to be spelled out in detail, although a qualitative picture can already be based on the average electron-wall impact energy. Experimental tests at the SPS will be conducted in the near future [19].

Build-up during the ramp

In this set of simulations we obtained the average n_e during the energy ramp, but only for one value of N_b, namely 1×10^{11}, corresponding to $N_t = 4.305 \times 10^{13}$ for the pattern "hi_int_mixed." In this case, the integration time step was $\Delta t = 2.5 \times 10^{-11}$ s, which is adequate. We also used a finer scan in $\delta_{\rm max}$ than in the above simulations.

Results are shown in Fig. 8. In general, one observes a weak dependence on E_k except possibly near transition, which can be explained by the short bunch length. This weak energy dependence is consistent with the microwave dispersion measurements but not with the RFA measurements, a discrepancy that remains to be fully explained. In all cases analyzed we observe again the threshold behavior of n_e as a function of $\delta_{\rm max}$, with a transition in $\delta_{\rm max} \sim 1.1 - 1.3$.

DISCUSSION

We have examined the electron cloud in the MI for a fill pattern made up of 6 trains, in which the bunch intensity in the 6th train is half of that in the previous 5. This pattern can be achieved in practice by slip-stacking booster

batches. We have examined pulse intensities in the range $N_t = (2-5)\times 10^{13}$, corresponding to bunch intensities (in the first 5 batches) in the range $N_b \simeq (0.4-1.1)\times 10^{11}$. The main conclusions from the results presented here are:

1. At fixed N_t, there is a clear threshold behavior of n_e as a function of $\delta_{\max}$ in the region $\delta_{\max} = 1.1-1.3$. This result is fully consistent with previous simulations we have carried out for the MI.

2. At fixed $\delta_{\max}$, there is also a threshold behavior of n_e as a function of N_t, provided $\delta_{\max}$ is high enough (typically $\gtrsim 1.3$). The threshold value of N_t depends on the details of the region being simulated: for "bend," $N_t < 2\times 10^{13}$; for "edet and "FFellip,", $N_t = (3-4)\times 10^{13}$. This result is qualitatively consistent with prior simulations.

3. The electron-cloud average density shows a weak dependence on beam energy except at transition. This qualitative feature is more consistent with the microwave dispersion measurements than with the RFA measurements.

4. When $\delta_{\max}$ is at or above the transition region, the simulations show deep fluctuations resulting from a "virtual cathode" effect. The fluctuations are partly physical and partly due to numerical artifacts, but do not significantly affect the one-turn averages of n_e. An improved simulation model is called for in order to better understand and control these effects.

ACKNOWLEDGMENTS

I am indebted to I. Kourbanis, N. Eddy and R. Zwaska for experimental results, many discussions and guidance.

REFERENCES

[1] Proton Driver Study. II. (Part 1, ch. 13), FERMILAB-TM-2169 (G. W. Foster, W. Chou and E. Malamud, eds.), May 2002.

[2] R. Zwaska, "Electron Cloud Studies in FNAL Main Injector," Proc. HB2008 (Nashville, August 25-29, 2008). http://neutrons.ornl.gov/workshops/hb2008/.

[3] I. Kourbanis, "e-Cloud MI Measurements", 26 Aug. 2007.

[4] N. Eddy, J. L. Crisp, I. Kourbanis, K. Seiya, R. M. Zwaska, S. De Santis, "Measurement of Electron Cloud Development in the Fermilab Main Injector Using Microwave Transmission," Proc. PAC09, paper WE4GRC02

[5] P. Lebrun, P. Stoltz, S. A. Veitzer, "Microwave Transmission through the Electron Cloud at the Fermilab Main Injector: Simulation and Comparison with Experiment," Proc. PAC09, paper TH5PFP019

[6] M. A. Furman, I. Kourbanis and R. M. Zwaska, "Status of Electron-Cloud Build-Up Simulations for the Main Injector," Proc. PAC09 (Vancouver, BC, 4-8 May 2009), paper TH5PFP032, LBNL-xxx. http://www.triumf.info/hosted/PAC09/

[7] M. A. Furman and G. R. Lambertson, "The electron-cloud instability in the arcs of the PEP-II positron ring," LBNL-41123/CBP Note-246, PEP-II AP Note AP 97.27 (Nov. 25, 1997). Proc. *Intl. Workshop on Multibunch Instabilities in Future Electron and Positron Accelerators "MBI-97"* (KEK, 15-18 July 1997; Y. H. Chin, ed.), KEK Proceedings **97-17**, Dec. 1997, p. 170.

[8] M. A. Furman and M. T. F. Pivi, "Probabilistic model for the simulation of secondary electron emission," LBNL-49771/CBP Note-415 (Nov. 6, 2002). PRST-AB **5** 124404 (2003), http://prst-ab.aps.org/pdf/PRSTAB/v5/i12/e124404.

[9] M. A. Furman and M. T. F. Pivi, "Simulation of secondary electron emission based on a phenomenological probabilistic model," LBNL-52807/SLAC-PUB-9912 (June 2, 2003).

[10] M. A. Furman, "The electron-cloud effect in the arcs of the LHC," LBNL-41482/CBP Note 247/LHC Project Report 180 (May 20, 1998).

[11] M. A. Furman, "ECLOUD in PS2, PS+, SPS+," LBNL-61925, CBP Note 762, Nov. 7 2006. Proc. LHC LUMI 2006 CARE-HHH-APD Workshop "Towards a Roadmap for the Upgrade of the CERN and GSI Accelerator Complex," (IFIC, Valencia, Spain, 16-20 October 2006), http://care-hhh.web.cern.ch/CARE-HHH/LUMI-06/default.html

[12] M. A. Furman, "A preliminary assessment of the electron cloud effect for the FNAL main injector upgrade," LBNL-57634/CBP-Note-712/FERMILAB-PUB-05-258-AD, 23 June 2006. A condensed version of this articled, of the same title, is published in New J. Phys. **8** (2006) 279. http://stacks.iop.org/1367-2630/8/279

[13] M. A. Furman home page, http://mafurman.lbl.gov

[14] I. Kourbanis, N. Eddy and R. M. Zwaska, private communication.

[15] M. A. Furman, "Electron-Cloud Build-Up Simulations for the FNAL Main Injector," LBNL-1402E/CBP Tech Note 387, Sept. 19, 2008. Proc. HB2008 (Nashville, August 25-29, 2008), http://neutrons.ornl.gov/workshops/hb2008/

[16] G. Rumolo, SPS Upgrade Study Team Mtg., Nov. 20, 2007, https://paf-spsu.web.cern.ch/paf-spsu/meetings/2007/M20-11/min9.pdf

[17] M. A. Furman, "PS2 Electron-Cloud Build-Up Studies: Status," LARP CM12, Napa (California), 9 April 2009.

[18] M. A. Furman, R. De Maria, Y. Papaphilippou and G. Rumolo, "Electron-Cloud Build-Up Simulations in the Proposed PS2: Status Report," LBNL-xxx/CBP-851, May 25, 2010, Proc. IPAC10 (Kyoto, Japan, May 23-28, 2010), paper TUPD018.

[19] G. Rumolo, private comunication.

DISCLAIMER

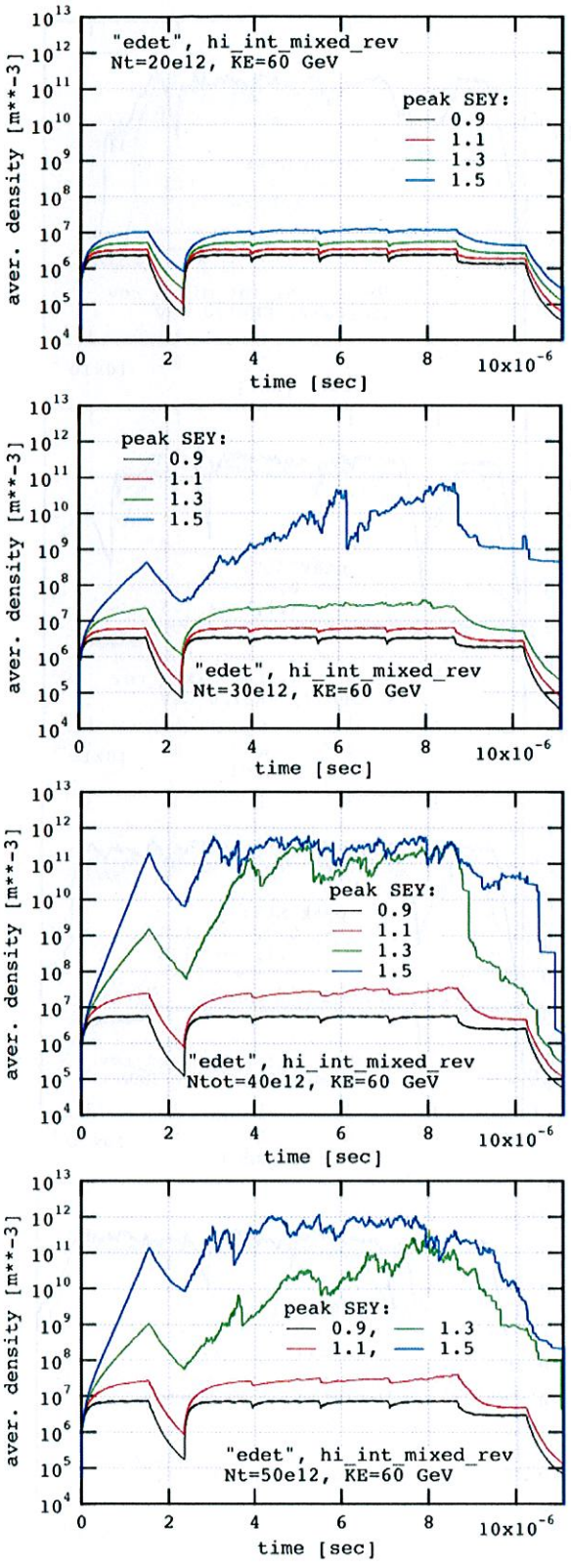

Figure 4: Build-up of the average ecloud density during one turn in a "edet" region, at $E_k = 60$ GeV, for the fill pattern "hi_int_mixed_rev" for $N_t = (2, 3, 4, 5) \times 10^{13}$, as labeled. Each trace corresponds to the indicated value of the peak SEY $\delta_{\max}$.

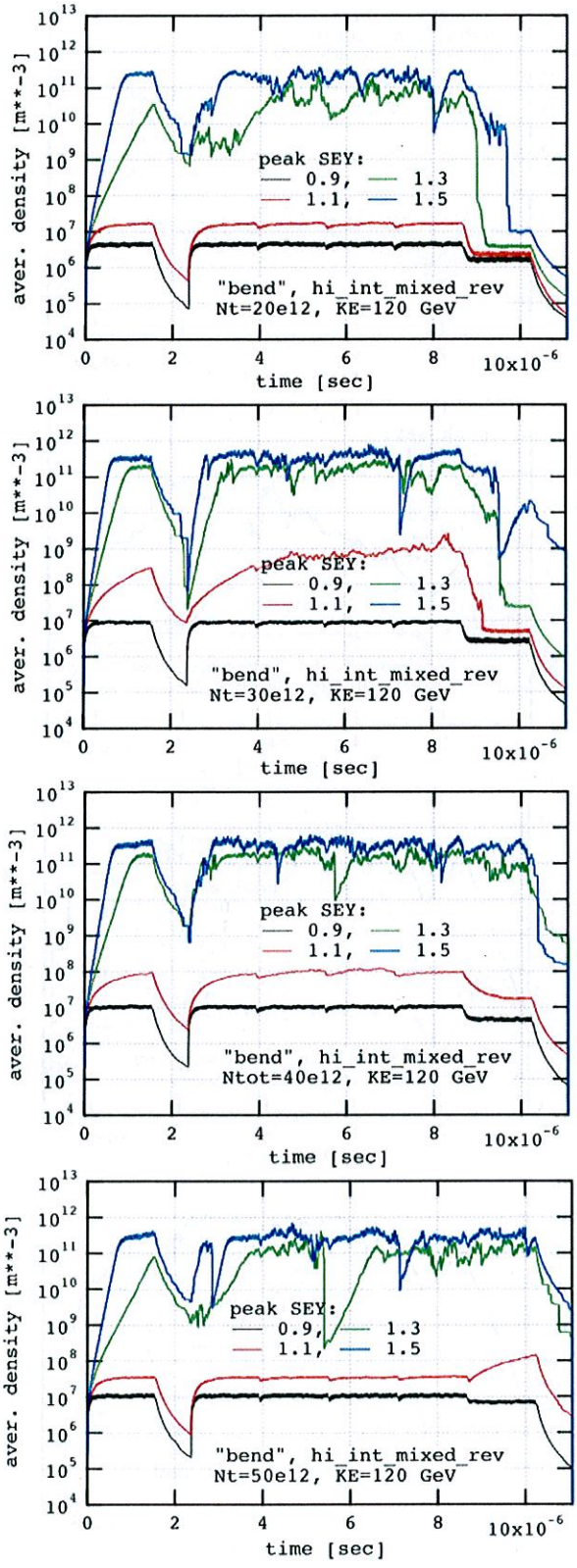

Figure 5: Build-up of the average ecloud density during one turn in a "bend" region, at $E_k = 120$ GeV, for the fill pattern "hi_int_mixed_rev" for $N_t = (2, 3, 4, 5) \times 10^{13}$, as labeled. Each trace corresponds to the indicated value of the peak SEY $\delta_{\max}$.

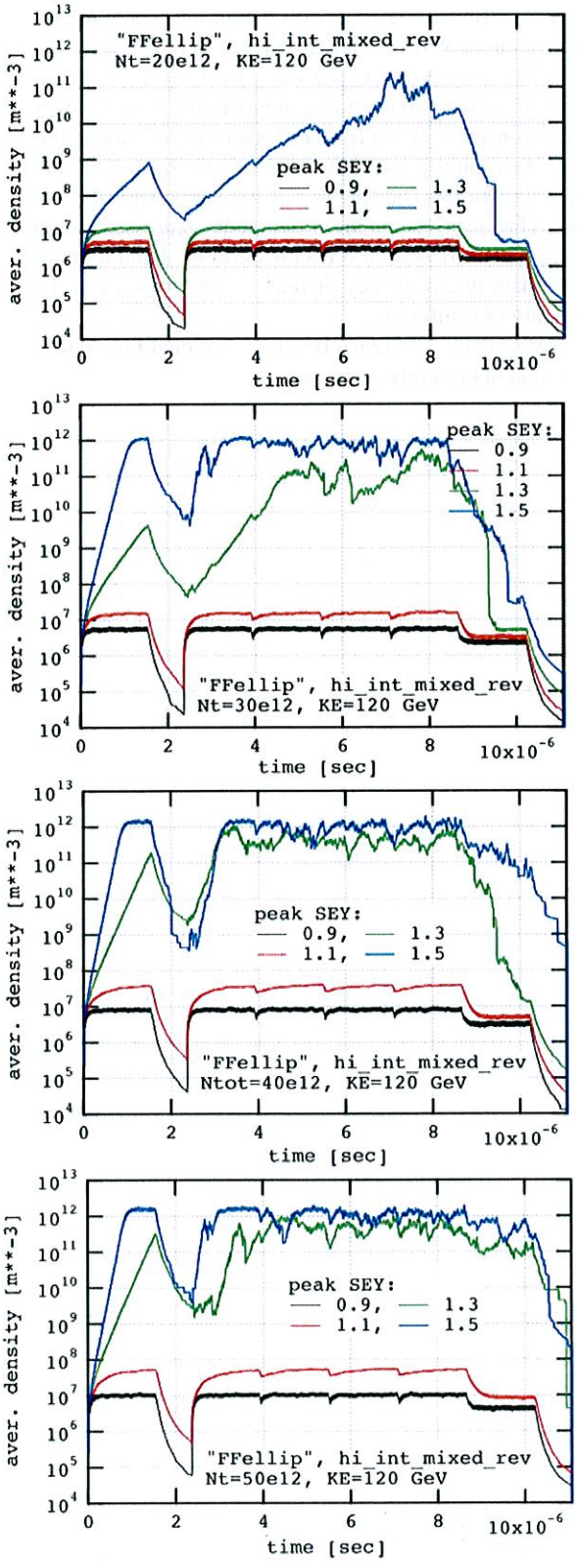

Figure 6: Build-up of the average ecloud density during one turn in a "FFellip" region, at $E_k = 120$ GeV, for the fill pattern "hi_int_mixed_rev" for $N_t = (2, 3, 4, 5) \times 10^{13}$, as labeled. Each trace corresponds to the indicated value of the peak SEY $\delta_{\max}$.

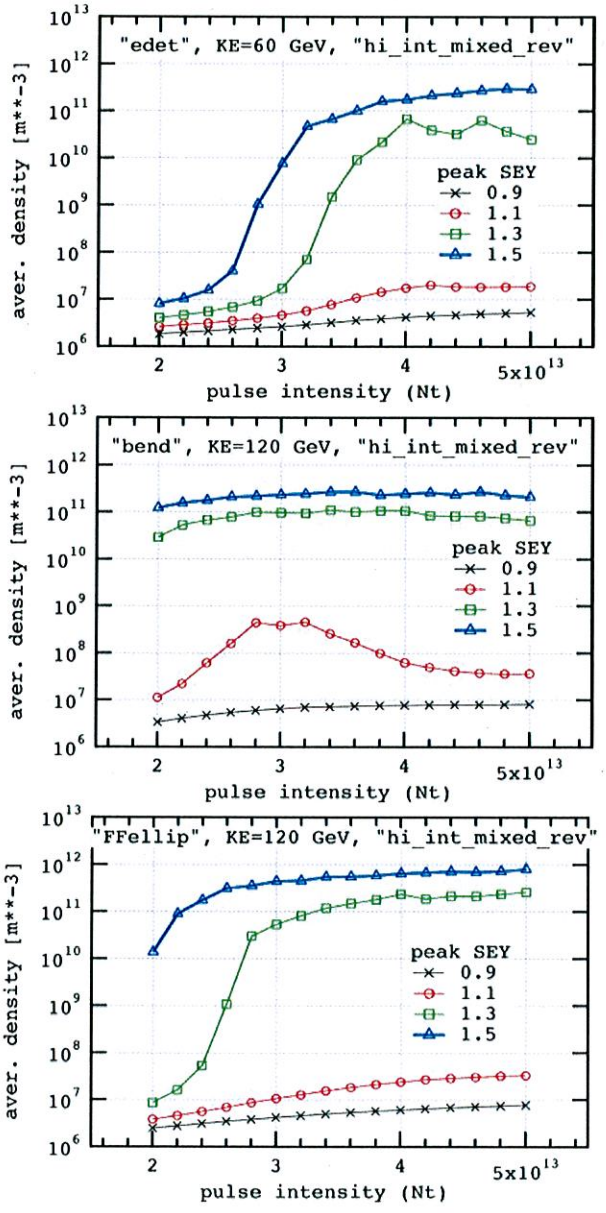

Figure 7: Average ecloud density at a given beam energy, as indicated, as a function of pulse intensity N_t for the pattern "hi_int_mixed_rev." Each trace corresponds to the indicated value of the peak SEY $\delta_{\max}$.

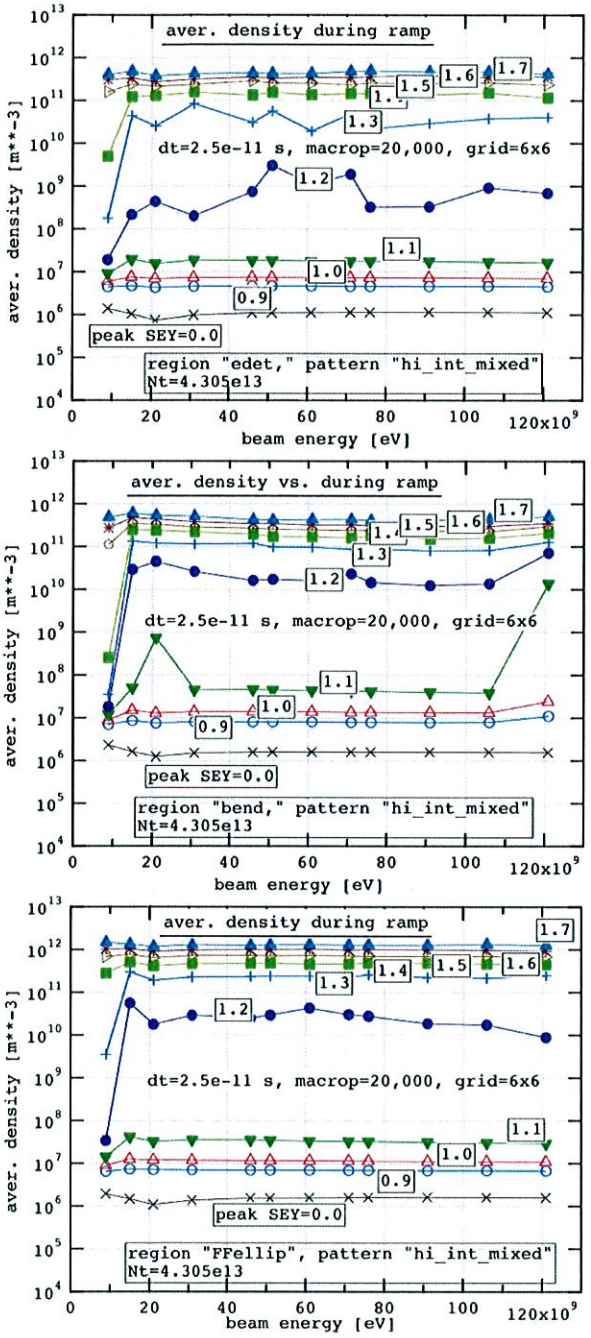

Figure 8: one-turn average of n_e during the ramp in each of the 3 regions simulated, for the fill pattern "hi_int_mixed" for $N_b = 1 \times 10^{11}$ ($N_t = 4.305 \times 10^{13}$). Each trace corresponds to the indicated value of the peak SEY $\delta_{\max}$. The abscissa is the full beam energy, $E_k + m_p c^2$.